University of Groningen

Infall of substructures on to a Milky Way-like dark halo

Li, Yang-Shyang; Helmi, Amina

Published in:
Monthly Notices of the Royal Astronomical Society

DOI:
10.1111/j.1365-2966.2008.12854.x

IMPORTANT NOTE: You are advised to consult the publisher's version (publisher's PDF) if you wish to cite from it. Please check the document version below.

Document Version
Publisher's PDF, also known as Version of record

Publication date:
2008

Link to publication in University of Groningen/UMCG research database

Citation for published version (APA):
Li, Y-S., & Helmi, A. (2008). Infall of substructures on to a Milky Way-like dark halo. *Monthly Notices of the Royal Astronomical Society*, *385*(3), 1365-1373. https://doi.org/10.1111/j.1365-2966.2008.12854.x

Copyright
Other than for strictly personal use, it is not permitted to download or to forward/distribute the text or part of it without the consent of the author(s) and/or copyright holder(s), unless the work is under an open content license (like Creative Commons).

The publication may also be distributed here under the terms of Article 25fa of the Dutch Copyright Act, indicated by the "Taverne" license. More information can be found on the University of Groningen website: https://www.rug.nl/library/open-access/self-archiving-pure/taverne-amendment.

Take-down policy
If you believe that this document breaches copyright please contact us providing details, and we will remove access to the work immediately and investigate your claim.

Downloaded from the University of Groningen/UMCG research database (Pure): http://www.rug.nl/research/portal. For technical reasons the number of authors shown on this cover page is limited to 10 maximum.

Download date: 04-05-2023

Mon. Not. R. Astron. Soc. **385,** 1365–1373 (2008) doi:10.1111/j.1365-2966.2008.12854.x

Infall of substructures on to a Milky Way-like dark halo

Yang-Shyang Li★ and Amina Helmi★

Kapteyn Astronomical Institute, University of Groningen, PO Box 800, 9700 AV Groningen, the Netherlands

Accepted 2007 December 10. Received 2007 December 10; in original form 2007 November 15

ABSTRACT

We analyse the dynamical properties of substructures in a high-resolution dark matter simulation of the formation of a Milky Way-like halo in a Λcold dark matter cosmology. Our goal is to shed light on the dynamical peculiarities of the Milky Way satellites. Our simulations show that about one-third of the subhaloes have been accreted in groups. We quantify this clustering by measuring the alignment of the angular momentum of subhaloes in a group. We find that this signal is visible even for objects accreted up to $z \sim 1$, i.e. 8 Gyr ago, and long after the spatial coherence of the groups has been lost due the host tidal field. This group infall may well explain the ghostly streams proposed by Lynden-Bell & Lynden-Bell to orbit the Milky Way. Our analyses also show that if most satellites originate in a few groups, the disc-like distribution of the Milky Way satellites would be almost inevitable. This non-random assignment of satellites to subhaloes implies an environmental dependence on whether these low-mass objects are able to form stars, possibly related to the nature of reionization in the early Universe. With this picture, both the 'ghostly streams' and the 'disc-like configuration' are manifestations of the same phenomenon: the hierarchical growth of structure down to the smallest scales.

Key words: methods: numerical – Galaxy: formation – galaxies: dwarf – galaxies: kinematics and dynamics – dark matter.

1 INTRODUCTION

In cold dark matter (CDM) cosmologies, large galaxies are the result of the aggregation of smaller subunits. Some of these subunits may survive until the present day in the form of satellites, while some may be completely destroyed in the course of time, and contribute to the field. In *N*-body CDM simulations of the formation of galaxy-size dark-matter haloes, the satellites (often referred to as substructures or subhaloes) show significantly different properties than those of the 'luminous' satellites around galaxies like the Milky Way (MW). An example of this discrepancy is the 'missing satellite problem': subhaloes outnumber the bright satellites by a factor of 100 or more (Kauffmann, White & Guiderdoni 1993; Klypin et al. 1999; Moore et al. 1999). Furthermore, their spatial distribution is typically much shallower than observed for the luminous satellites (Gao et al. 2004a; Taylor, Babul & Silk 2004). Therefore, the relation between resolved substructures/subhaloes in dark matter simulations and the luminous satellites in galaxy haloes is still unclear. Attempts to reconcile these two populations, using semi-analytic models of galaxy formation (Kauffmann, White & Guiderdoni 1993; Benson et al. 2002; Kravtsov, Gnedin & Klypin 2004) or full-fleshed smoothed particle hydrodynamics (SPH)-simulations (Macciò et al. 2006; Libeskind et al. 2007) have produced interesting results, and helped us gain insight into the relevant processes on the smallest galactic scales.

In the past 10 years, new attention has been drawn to the properties of the satellite population in the Local Group. Starting with Lynden-Bell & Lynden-Bell (1995), the existence of ghostly streams of satellites (dwarf galaxies and globular clusters) was proposed. These objects would share similar energies and angular momenta producing a strong alignment along great circles on the sky (Palma, Majewski & Johnston 2002). Recently, it has been argued that the MW satellites define a disc-like structure, that is, so highly flattened (rms thickness of 10–30 kpc) that may at first sight be inconsistent with CDM models (Kroupa, Theis & Boily 2005; Metz, Kroupa & Jerjen 2007). However, sophisticated modelling combining semi-analytic galaxy formation recipes with dark matter simulations has produced results that are consistent with observations (Kang et al. 2005; Libeskind et al. 2005; Zentner et al. 2005).

In the past two years, about a dozen low-surface brightness dwarf satellite galaxies around the MW have been found in the Sloan Digital Sky Survey (SDSS) (Willman et al. 2005a,b; Belokurov et al. 2006; Zucker et al. 2006a,b; Belokurov et al. 2007; Irwin et al. 2007). This is an increase by a factor of 2 in the number of known satellites. Because of the strong selection bias (SDSS focus is on the north galactic pole), it is unclear whether these satellites confirm the flattened disc-like structure. It is also unclear whether they help solve the missing satellite problem (Simon & Geha 2007). Satellites around M31 also show peculiarities in their distribution, such as an

★E-mail: ysleigh@astro.rug.nl (Y-SL); ahelmi@astro.rug.nl (AH)

© 2008 The Authors. Journal compilation © 2008 RAS
Downloaded from https://academic.oup.com/mnras/article-abstract/385/3/1365/1010777 by University of Groningen user on 28 June 2018

excess of objects on the side closest to the MW (McConnachie & Irwin 2006), and possibly a similar degree of alignment (Koch & Grebel 2006).

These facts have motivated us to revisit the distribution and properties of the subhalo population in CDM simulations. In particular, here we focus on the infall of substructures on to a MW-like dark matter halo in a ΛCDM cosmogony. We use a high-resolution dark-matter simulation that is a variant of the GA series (Stoehr et al. 2002; Stoehr 2006) as described in Section 2.1. We find evidence of group infall on to the MW-like halo, which may explain the ghostly streams proposed by Lynden-Bell & Lynden-Bell (1995). This is discussed in Section 2.2. In Section 2.3, we show that the disky configuration of satellites is consistent with CDM if most satellites have their origin in a few groups. Thus, both the 'ghostly streams' and the 'planar configuration' are manifestations of the same phenomenon: the hierarchical growth of structure down to the smallest galactic scales. We present our conclusions in Section 3.

2 SUBHALOES IN THE DARK MATTER SIMULATIONS

2.1 Description of the simulations

We have analysed the GAnew series of high-resolution simulations of a MW-like halo (Stoehr 2006). The simulations were carried out with GADGET-2 (Springel et al. 2001). The halo was selected from the M3 ΛCDM series (see Ciardi, Stoehr & White 2003) with cosmological parameters $\Omega_0 = 0.3$, $\Omega_\Lambda = 0.7$, $h = 0.7$, and Hubble constant $H_0 = 100$ h km s^{-1} Mpc^{-1}. Candidate haloes in this simulation were selected according to the following criteria: (i) well resolved, with >500 particles, (ii) environment similar to the Local Group (free from nearby rich galaxy clusters), (iii) peak circular velocity approximately 220 km s^{-1} and (iv) no major merger since $z = 2$ (see Gilmore, Wyse & Norris 2002). After choosing the best MW-like halo, the zoomed initial conditions technique (Tormen, Bouchet & White 1997) was used to produce a higher resolution simulation. The MW-like halo was simulated four successive times with the mass resolution increased by a factor of 9.33 each time. In the highest mass-resolution simulation (GA3new), there are approximately 10^7 particles within the virial radius. Each of these re-simulations produced 60 outputs equally spaced in $\log[1/(1+z)]$ between $z = 37.6$ and 0. Table 1 summarizes the parameters and properties of the GAnew series.

Verbalized structures were identified in the high-resolution region of the simulation using the standard friends-of-friends algorithm linking particles separated by less than 0.2 of the mean interparticle separation. The SUBFIND algorithm (Springel et al. 2001) was then applied to each FOF group to find the gravitationally self-bound subhaloes. The smallest resolved subhalo contains 10 particles, and its mass is $\sim 2.7 \times 10^7\,\mathrm{M}_\odot$ in GA2new and $\sim 2.9 \times 10^6\,\mathrm{M}_\odot$ in GA3new. The number of subhaloes present in the final output is 504 for GA2new and increases to 3892 for GA3new. The virial mass of the MW-like halo is $2.4 \times 10^{12}\,h^{-1}\,\mathrm{M}_\odot$ and the virial radius is $R_{\rm vir} = 217\,h^{-1}$ kpc at present time in GA3new.

Table 1. Numerical parameters for the GAnew-series simulations. The number of low-resolution particles remains at a roughly constant level of $nlr \sim 1.272 \times 10^6$.

Name	$m_{\rm p}(h^{-1}\,\mathrm{M}_\odot)$	$N_{\rm HR}$	$z_{\rm start}$	$\epsilon(h^{-1}$ kpc)
GA0new	1.677×10^8	68 323	70	1.4
GA1new	1.796×10^7	637 966	80	0.8
GA2new	1.925×10^6	5 953 033	90	0.38
GA3new	2.063×10^5	55 564 205	60	0.18

2.2 Group infall of dark matter substructures

2.2.1 *Infall pattern*

The bottom panels of Fig. 1 show the present-day spatial distribution of subhaloes accreted at four different redshifts ($z_{\rm acc}$) in GA3new. We use the most bound particle of a subhalo to represent its position and velocity. The accretion epoch of a subhalo is determined as the time when its most bound particle becomes part of the FOF group in which the MW-like halo is located. The reference frame used in Fig. 1 is defined by the principal axes of the MW-like halo. Its principal axes have been determined by diagonalizing the inertia tensor:

$$I_{ij} = \sum_\mu x_i^\mu x_j^\mu / \zeta_\mu^2, \tag{1}$$

where x_i^μ is the i coordinate of the μth particle with respect to a reference frame centred on the main halo, $\zeta_\mu^2 = (y_1^\mu)^2 + (y_2^\mu/s)^2 + (y_3^\mu/q)^2$ and y_i^μ are its coordinates in the principal axes frame (Dubinski & Carlberg 1991; Zentner et al. 2005). We only consider particles with $\zeta^2 \leqslant R_{\rm vir}$, and iterate until s and q have changed by less than $\sim 10^{-3}$. The present time minor-to-major axis ratio of the MW-like halo is $q = 0.6$, and it has changed by less than 5 per cent over the last 3 Gyr.

The top row of Fig. 1 shows the spatial distribution of subhaloes at the time they were accreted on to the MW-like halo. The (grey) dashed circles in top panels show the virial radius at that epoch. There are 789, 231, 133 and 117 subhaloes which have survived until present time that were accreted at $z = 0.06$, 0.28, 0.63 and 1.08, respectively. Note that in the first column, we plot for clarity only the first 200 most massive subhaloes accreted at $z_{\rm acc} = 0.063$.

The distribution of subhaloes is elongated roughly along the direction of the major axis of the MW-like halo at each epoch. The projected major axis orientations of subhaloes accreted at a given epoch are indicated by the dashed lines in Fig. 1. These are computed using equation (1) but without resampling.[1] The alignment between the host and the subhalo's major axes is prominent except for the $z_{\rm acc} = 0.28$ snapshot. At this time the accreted subhaloes are much more isotropically distributed, preventing a clean determination of the orientation of the principal axes of inertia (since the intermediate-to-major axis ratio is 0.98).

Fig. 1 also shows that the distribution of subhaloes is clumpy on small scales. These clumps are formed by subhaloes sharing similar velocities (as shown by the arrows in this figure). This indicates that infall does not occur in isolation but in groups. This is very reminiscent of the way that clusters of galaxies grow through the mergers of groups, residing in the intersections of filaments (e.g. Knebe et al. 2004). What we are seeing here is that also galaxy-size haloes grow via accretion of 'subgroup'-size structures.

The clumps of subhaloes seen in Fig. 1 share essentially the same angular momentum at the time of infall. This implies that, even if the spatial clustering is less prominent after a few orbits inside the main halo, the lumpiness may still be present in the space of angular momenta, provided these are nearly conserved.

[1] When the number of subhaloes is small, as in the right-hand panel of Fig. 1, an iterative procedure quickly leads to a sample with too few points, and hence to unreliable results.

Downloaded from https://academic.oup.com/mnras/article-abstract/385/3/1365/1010777
by University of Groningen user
on 28 June 2018

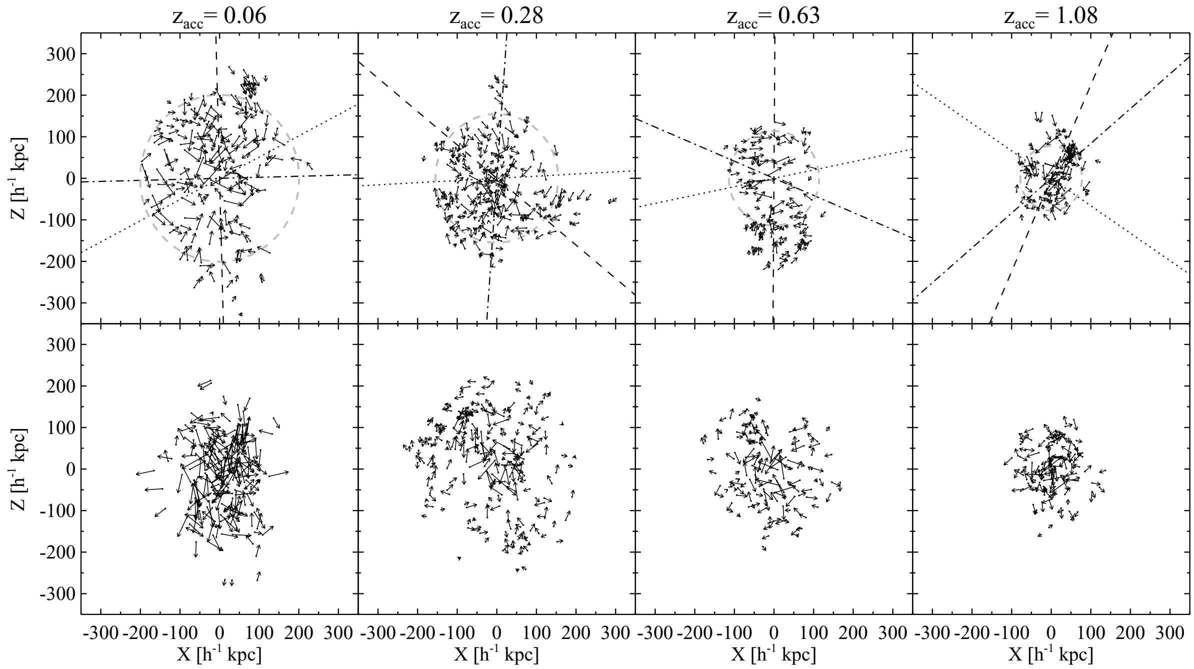

Figure 1. Distribution of present-day subhaloes in the MW-like halo in GA3new. The top panels show their distribution at the redshift of accretion $z_{\rm acc}$ in the principal axis reference frame defined by the main halo at that epoch, while the bottom panels correspond to the present day. The arrows represent the velocity vector of each subhalo: its length corresponds to 0.15 of the velocity magnitude while the orientation is defined by the direction of motion. The dashed, dash dot and dotted lines in each panel indicate the directions of the major, intermediate and minor axes of the ellipsoid defined by these subhaloes. The circle denotes the virial radius of the host at the accretion epoch. Several groups of subhaloes can be seen in these diagrams, in particular, at the time of accretion.

We quantify the degree of clustering by computing the two-point ‘angular correlation function’, $\omega(\alpha)$, of the present-day angular momentum of our subhaloes. The angle α is defined by the relative orientation of the angular momenta of any two subhaloes, i.e. $\cos\alpha_{ij} = \boldsymbol{L}_i \cdot \boldsymbol{L}_j/(|\boldsymbol{L}_i||\boldsymbol{L}_j|)$. Therefore, the correlation function ω measures the number of pairs with $\alpha_{ij} < \alpha$ compared to the expectations of an isotropic distribution. To compute the expected number of random pairs, we average over 1000 realizations of a uniform distribution on the sphere, whose size is given by the number of ‘observed’ data points. Note that any small-scale clustering in angular momentum such as observed in Fig. 1 should manifest itself as an excess of pairs with small angular separations.

Fig. 2 shows the two-point ‘angular correlation function’ computed using the present-day angular momentum of subhaloes in our simulations. Different colours correspond to subhaloes accreted at different epochs. We see a clear excess of pairs with angular momentum orientation separation less than 10° (and up to 30°) compared to random samples. This implies that the signature of group infall is preserved in angular momentum even after many Gyr of evolution. This signal is still discernible even for subhaloes accreted at $z \sim 1$. The correlation function calculated with all surviving subhaloes at present is showed as the (black) dashed line.

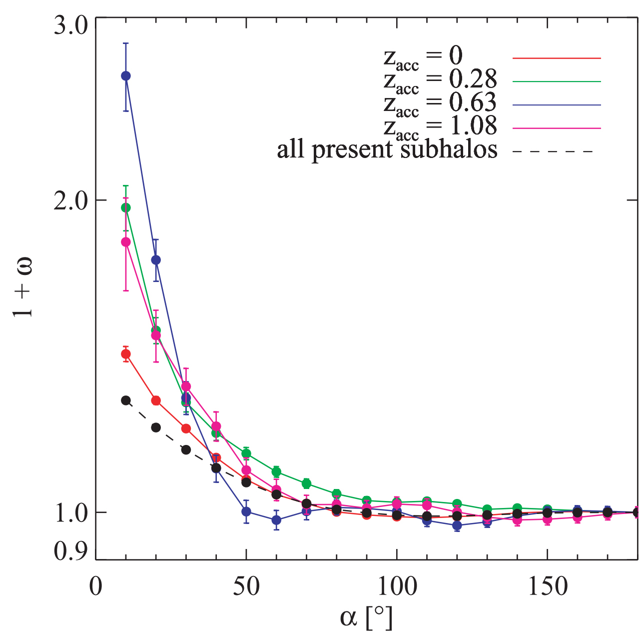

Figure 2. Two-point ‘angular correlation function’ using the present time angular momentum orientation of subhaloes accreted in the last 8 Gyr. The excess in the first bins is indicative of the group infall, and shows that this signal can persist for a very long time.

2.2.2 *Properties of groups*

We now focus on the characteristics of the groups accreted at the various epochs. To identify groups, we link pairs of infalling haloes whose angular momentum orientations are separated by $\alpha < 10°$ and with relative distances $d < 40$ kpc at the time of accretion. We found that this combination of α and d values results in a robust set of groups, maximizing their extent while minimizing the number of spurious links.

We follow the orbits of the groups identified from redshift $z \sim 4.2$ until present time. Fig. 3 shows the trajectories of some of the richest groups of subhaloes, which were accreted 2.43, 1.65 and 0.84 Gyr ago, respectively. Each dot represents the position of a

Downloaded from https://academic.oup.com/mnras/article-abstract/385/3/1365/1010777
by University of Groningen user
on 28 June 2018

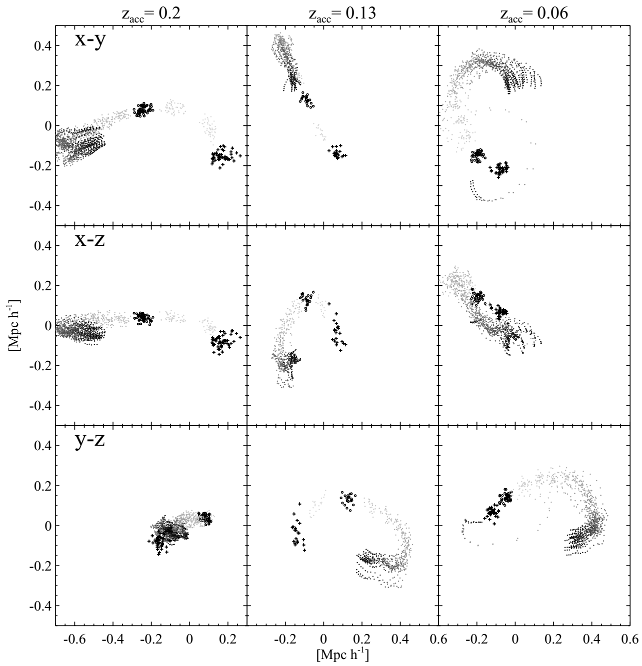

Figure 3. Three examples of the trajectories of groups of subhaloes accreted at different epochs in the GA3new simulation reference frame. These are some of the most abundant groups ever accreted. The colour gradients indicate the arrow of time, from dark at high redshift to light grey at the present. The positions at accretion and present time are highlighted with open circles and crosses, respectively. There is some evidence that these groups themselves are the result of the mergers of smaller groups, this is especially clear for the group in the right most panel.

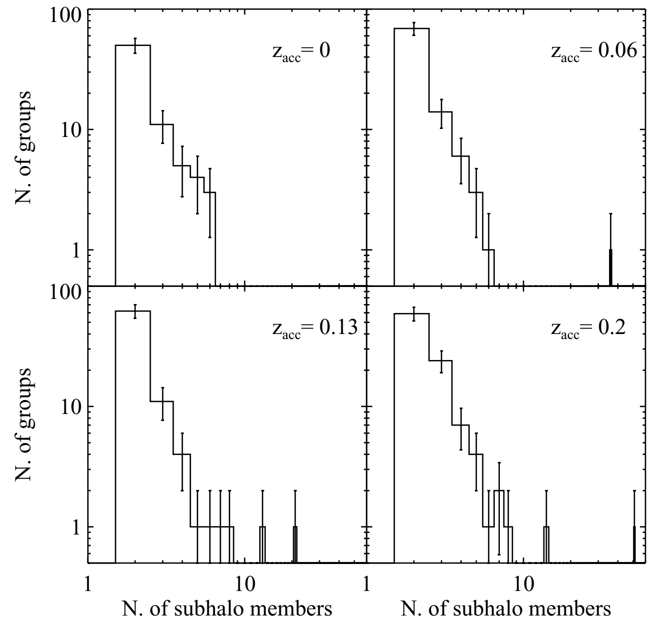

Figure 4. Number counts of groups as function of the number of member subhaloes at four accretion epochs plotted in log–log scale. The errorbars are Poissonian.

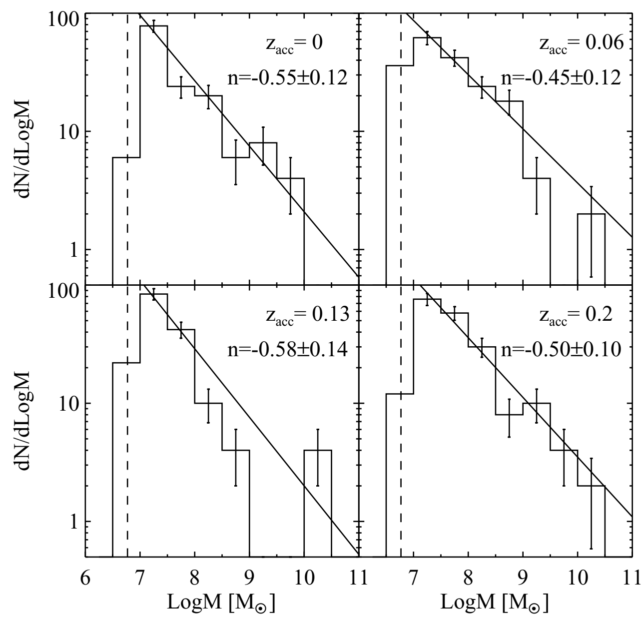

Figure 5. Differential mass function of the groups shown in Fig. 4. The power-law behaviour of the group mass function is similar to that of the subhalo mass function, albeit with a shallower slope.

subhalo colour coded from high redshift (dark) to the present (light grey). The crosses correspond to the present-day positions while those at the time of accretion are shown as open circles. Fig. 3 clearly shows that the groups of subhaloes follow nearly coherent orbits as early as $z \sim 4.2$, long before the time of accretion.

The characteristic size of the groups can be measured by computing the number function of groups, i.e., how many groups have a given number of subhaloes. Fig. 4 shows the number function of groups accreted in the four most recent snapshots: present time, 0.84, 1.65 and 2.43 Gyr ago. As can be seen from this figure, the shape is quite similar at all times, and most of the groups have a small number of members.

Fig. 5 shows the differential mass function of the groups in Fig. 4 down to our resolution limit (the dashed line, which corresponds to $\sim 5.89 \times 10^6\,M_\odot$). Once again we find very similar power-law shapes for the mass functions at different epochs. This power-law shape is reminiscent of the differential mass function of subhaloes in cluster and galaxy-size dark matter haloes. The slope of the fitted $dN/d\log M \propto M^n$ relation is $n \sim -0.5 \pm 0.2$. Note that this is somewhat shallower than that found for subhaloes, where $n \sim -0.8 \pm 0.1$ (Stoehr et al. 2003; De Lucia et al. 2004; Gao et al. 2004b). This could be well due to insufficient mass resolution: the fact that we are not resolving subhaloes below $2.9 \times 10^6\,M_\odot$, implies that many subhaloes are accreted in isolation, instead of in pairs or in groups. This effect is much stronger at the low-mass end of the group mass spectrum. For example, a group with total mass $\sim 10^9\,M_\odot$ can consist of 10 subhaloes of $\sim 10^8\,M_\odot$ or two of $\sim 5 \times 10^8\,M_\odot$. On the other hand, a group of $\sim 10^7\,M_\odot$ can only be the result of a pair of subhaloes of $5 \times 10^6\,M_\odot$ in our simulation.

Our limited resolution also prevents us from quantifying the mass function inside the groups. Nevertheless, and for our largest groups, we find that these are dominated by a few massive subhaloes and many small ones.

The group infall that we have been detecting in our simulation may be well related to the ghostly streams reported by Lynden-Bell & Lynden-Bell (1995). The presence of satellites (dwarf galaxies and globular clusters) sharing a common orbital plane seems rather plausible in the context discussed here. Instead of the disruption of

Downloaded from https://academic.oup.com/mnras/article-abstract/385/3/1365/1010777
by University of Groningen user
on 28 June 2018

a large progenitor (Lynden-Bell & Lynden-Bell 1995) or the tidal formation of satellites within gas-rich major mergers (Kroupa 1997), we would be witnessing the disruption by the tidal field of the MW of a 'subgroup'-size object composed by dwarf galaxies. The possible implications of this finding are discussed in the conclusions.

2.2.3 *Link to the environment*

The present-time distribution of angular momentum orientations of subhaloes reflects both the anisotropy of the accretion pattern and the dynamical processes that affect subhaloes while orbiting the MW-like halo. Fig. 6 shows the orientation of the angular momentum of subhaloes accreted in the last 13 snapshots, from the present day (top left-hand panel) to $z \sim 1.08$ (bottom left-hand panel). Here, the angular momentum is calculated using the position and velocity of a subhalo in the simulation box frame right before it was accreted. Note that only a fraction of these subhaloes will have survived until the present time. The small-scale clustering visible in this figure once again highlights the group infall. Note the presence of larger scale patterns lasting over several snapshots (in particular, in the top row, which corresponds to the last 2.4 Gyr). This presumably implies that the infall patterns are related with persistent larger scale structures (filaments) in the tidal field.

To understand this in more detail, we proceed to trace the evolution of the tidal field around the main halo in our simulation. To this end, we select 'field' particles, i.e. those that do not belong to the FOF group of the MW-like halo. The projected spatial distribution of these particles within a $2\,h^{-1}$ Mpc on a side box is shown in grey in Fig. 7. Like in Fig. 6, each panel corresponds to a different redshift, starting from $z \sim 1.08$ in the bottom left-hand panel to the present day in the top left-hand panel. The distributions of surviving subhaloes accreted at the corresponding epoch are overplotted in black.

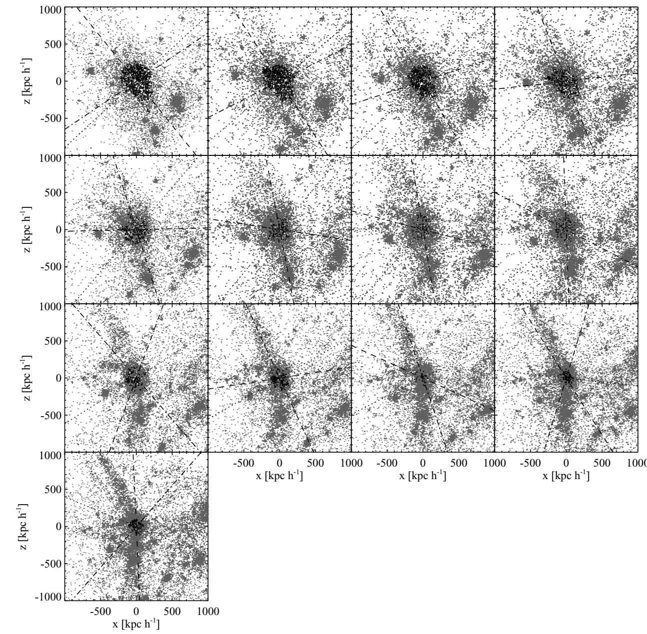

Figure 7. Evolution of the tidal field around the MW-like halo. The grey dots represent 0.05 per cent of the 'field' particles within a box of $2\,h^{-1}$ Mpc on a side in the simulation reference frame. Like in Fig. 6, the top left-hand panel corresponds to the present time, while the bottom left-hand panel to $z \sim 1.08$. The black circles denote the location of the subhaloes accreted at the given epoch. The dashed, dash–dot and dotted lines indicate the major, intermediate and minor axes of the MW-like halo at each epoch.

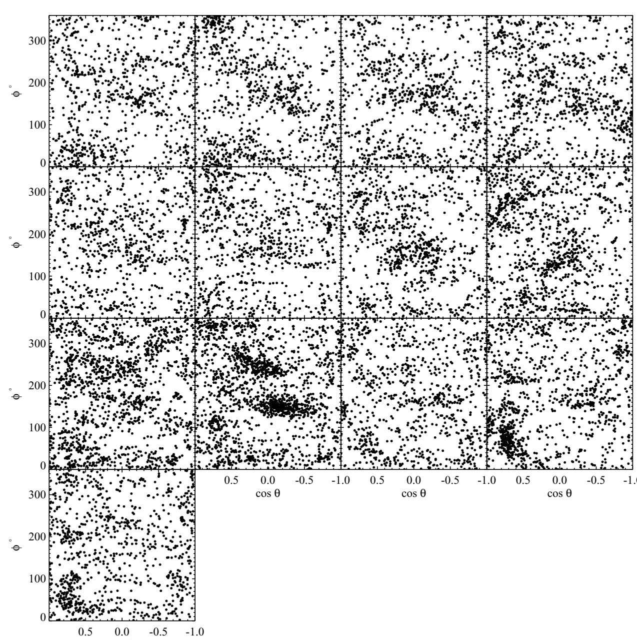

Figure 6. Distribution of angular momentum orientation for the subhaloes accreted in the last 13 snapshots, i.e. since $z = 1.08$. The arrow of time in this figure goes from right- to left-hand panel and from bottom to top panel, i.e. the bottom left-hand panel corresponds to ∼8 ago, while the top left-hand panel to the present day. Note the small-scale structure indicative of group infall as well as the large-scale pattern associated to the filamentary structure of the tidal field. This figure shows that not just one filament is actively feeding material at any given time.

Fig. 7 shows that the MW-like halo is embedded in a larger scale filamentary pattern. These filaments are comparable in extent to the halo itself (as e.g. traced by the accreted subhaloes). The lumpy nature of the filaments is also clearly visible, showing that the infall is not a continuous flow, but is in groups as discussed above.

Note that the global orientation of the tidal fields near the main halo has not changed much over the last four snapshots, in agreement with what is observed in the top row of Fig. 6. Furthermore, this large-scale pattern is more or less aligned with the major axis of the main halo, shown by the dashed line in each panel (as in Bailin & Steinmetz 2005).

2.3 On the great disc of Milky Way satellites

Kroupa et al. (2005) and Metz et al. (2007) have recently argued that the highly anisotropic distribution of MW satellites could not have been drawn from a nearly spherically distributed subhalo population. Motivated by their claim and the results presented above, we wish to test here under what conditions such a configuration is likely in a ΛCDM simulation like ours.

There are many possible ways to define the degree of flattening of a distribution. We will here concentrate on the following two measures.

(i) The minor-to-major axis ratio *c/a* derived from the eigenvalues of the diagonalized inertia tensor defined by the satellites positions.

(ii) The rms of the distances to the best-fitting plane to the satellites positions normalized by their median distance from the centre: $\Delta = D_{\rm rms}/R_{\rm med}$ (Kroupa et al. 2005; Zentner et al. 2005).

Downloaded from https://academic.oup.com/mnras/article-abstract/385/3/1365/1010777
by University of Groningen user
on 28 June 2018

In what follows the positions are defined with respect to the centroid of the satellites (or subhaloes), rather than with respect to the centre of the MW(-like) halo. For the first measure (i), we use the inertia tensor defined as

$$I^{\star}_{ij} = \sum_{\mu} x^{\mu}_i x^{\mu}_j. \qquad (2)$$

Note this inertia tensor differs from that previously used in equation (1) in which the positions were normalized by their ellipsoidal distance. Our preference for this new definition is based on the fact that the determination of the ellipsoidal distance is simultaneous to the determination of the eigenvalues of the inertia tensor I_{ij}. This means that an iterative algorithm is used, in which outliers are successively discarded, until the desired level of convergence is reached (see Section 2.2). However, when a relatively limited number of data points is available (as in the case of the MW satellites) this is clearly not desirable. Note as well that the shape of $I^{\star}_{ij}$ is more sensitive to objects at large distances. However, the effect this has on the measured *c/a* can be quantified, as we will see below.

In our analysis, we will only consider the 11 'traditional' MW satellites. This enables us to make a direct comparison to the work of Kroupa et al. (2005). On the other hand, it ensures we are not affected by the strong observational bias in the sky distribution of the new satellites discovered by SDSS, which reflects the fact that this survey has concentrated on the north galactic cap.

The minor-to-major axis ratio for the set of 11 'traditional' MW satellites is $c/a \sim 0.18 \pm 0.01$ where the uncertainty is due to errors in the Galactocentric distance (which also includes the uncertainty in the distance from the Sun to the Galactic Centre, $R_{\odot} = 8.0 \pm 0.5$ kpc). The plane containing the major and intermediate axes is inclined $72.8 \pm 0\overset{\circ}{.}7$ with respect to the Galactic disc, in good agreement with the value found by Metz et al. (2007).

If we use measure (ii) to quantify the degree of flattening, we find that the best-fitting plane of the MW satellites has an orientation identical to that of the inertia tensor. The rms distance to this plane is $D_{\rm rms} \sim 18.5$ kpc and the plane is offset from the Galactic Centre by 7.83 kpc. The median distance of the satellites is ∼80 kpc, which implies that $\Delta = 0.23 \pm 0.01$ assuming Gaussian errors of all related distances (see also Metz et al. 2007).

2.3.1 Overall distribution of subhaloes

The subhaloes in our GAnew simulations show at least two differences in their distributions in comparison to the Galactic dwarfs: (i) their spatial distribution is much less anisotropic and (ii) their density distribution is much shallower.

The present-day subhalo population of the MW-like halo has a minor-to-major axis ratio $c/a \sim 0.77$, obtained using equation (2), compared to $c/a = 0.74$ for the MW-like halo itself. These values are fairly consistent with those published by Zentner et al. (2005) and Libeskind et al. (2005). The minor-to-major axis ratio for those subhaloes within ∼300 kpc is $c/a \sim 0.86$. All these values are significantly larger than the $c/a \sim 0.18$ found for the MW satellites.

We now wish to test the effect of small number statistics in the determination of the principal axes of the inertia tensor. To this end, we randomly select 10^5 samples of N subhaloes: (i) from the simulated MW-like halo population; (ii) from an isotropic distribution with the same radial profile as found in the simulation. In Fig. 8, we plot the mean *c/a* as a function of the number N of subhaloes selected. The grey dots correspond to those drawn from present-day subhalo population (case i) while the black points are drawn from an isotropic sample (case ii). The errorbars denote the standard deviations of the 10^5 realizations. This figure shows that only when $N \sim 10^3$, a reliable estimate of the shape of the parent distribution can be obtained. The mean *c/a* tends to become smaller, that is, the distribution appears more flattened as the number of subhaloes becomes smaller. This is also true when the parent distribution is completely isotropic. When only 11 subhaloes are selected, the mean $c/a \sim 0.51 \pm 0.12$ ($c/a \sim 0.52 \pm 0.12$ for the isotropic case), quite different from that of the parent sample. Nevertheless, this is still significantly larger than observed for the MW satellites.

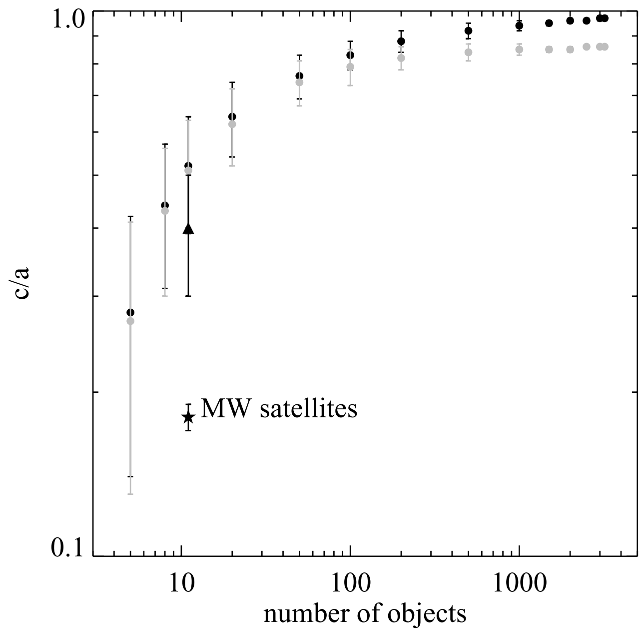

Figure 8. Minor-to-major axis ratio of the inertia tensor defined by random sets containing a varying number of subhaloes. The grey dots are for present-day subhaloes within 300 kpc in GA3new, while the black dots have been drawn from an isotropic distribution. The errorbars show the 1σ level of each distribution. The *c/a* obtained by imposing that 11 subhaloes follow the MW satellites, radial distribution is denoted by the triangle, while the star symbol corresponds to the *c/a* for the 11 MW satellites.

We noted previously that the density distribution of the satellites of the MW is strongly centrally concentrated. The median radius of the satellite's distribution is ∼80 kpc, comparable to the half-mass radius of the MW ($0.29\, r_{\rm vir}$ for a concentration of $c = 18$ as in Battaglia et al. 2005). On the other hand, the median radius for the subhaloes (within 300 kpc) in our simulation is much larger, $R_{\rm med} \sim 0.64 r_{\rm vir}$.

We now quantify the effect of this highly centrally concentrated distribution on the shape of the inertia tensor. We proceed by randomly selecting sets of 11 subhaloes from our simulation, but now imposing they follow the observed MW satellites spherically averaged spatial distribution. The mean minor-to-major axis ratio obtained in this way is $c/a \sim 0.40 \pm 0.10$, and is denoted as a triangle in Fig. 8. This exercise shows that the disc-like configuration of the MW satellites is indeed partially driven by their strongly centrally concentrated density distribution around the Galaxy (see also Kang et al. 2005; Zentner et al. 2005, for a similar discussion). However, this is still only marginally consistent with the MW satellites, i.e. the mean *c/a* of 10^5 11-random subhalo realizations is $\sim 2.2\sigma$ away from that observed.

Downloaded from https://academic.oup.com/mnras/article-abstract/385/3/1365/1010777
by University of Groningen user
on 28 June 2018

2.3.2 *Distribution of grouped subhaloes*

Inspired by the group infall of subhaloes found in Section 2.2, we now explore how the presence of such groups of subhaloes can affect the chance of obtaining a flattened configuration. Naively, we would expect that if their angular momenta is nearly conserved, the subhaloes would spread along their orbit and give rise to a planar structure as observed.

Given the large sensitivity of *c/a* to sample size, we prefer to use the Δ measure in what follows. This measure intuitively appears to be more robust since it derives from a simple plane fit to a distribution of points.

Of the 3246 subhaloes within 300 kpc from the centre of the MW-like halo that have survived until the present day, 898 subhaloes fell in as part of a group. 321 different groups have contributed to the present-day population of subhaloes, of which the earliest two were accreted at $z = 3.05$. From now on, subhaloes identified to be part of a group are referred to as 'grouped', while those which are not are termed 'field' subhaloes.

We first test how often a disc-like structure is obtained when selecting a set of 11 subhaloes consisting of a certain number $N_{\rm sub}$ of subhaloes from one group ($N_{\rm group} = 1$) while the rest $N_{\rm field}$ are from the 'field'. Note that $N_{\rm sub} = 2, 3, \ldots, 11$, and the condition $N_{sat} = N_{\rm field} + N_{\rm sub} = 11$ has to be satisfied. We make 10^5 realizations of such subsets and compute the fraction that gives rise to a configuration as flat as observed, i.e. $\Delta \leqslant 0.23$. The result is shown in the left-hand panel of Fig. 9 where the disc fraction increases from 4.5 per cent to 73 per cent as the number of selected subhaloes $N_{\rm sub}$ increases from 2 to 11. In comparison, 11-randomly selected subhaloes (within 300 kpc) give rise to flattened configurations $\sim$2.2 per cent of the time. This shows that if the MW satellites fell in together, it would not be very surprising that they would be in a planar configuration at the present day.

It is important to note that when $N_{\rm sub} \geqslant 6$, we select predominantly from just two groups accreted at relatively high redshift ($z = 1.08$ and 0.84). Other large groups accreted more recently are still strongly clustered in space, and hence are discarded in this exercise since they cannot be considered as a valid representation of the MW satellite population. Furthermore, although there is a relatively high chance of obtaining a value of Δ as low as observed, this is driven more by the large median distance of the subhaloes than by their rms distance to the best-fitting plane.

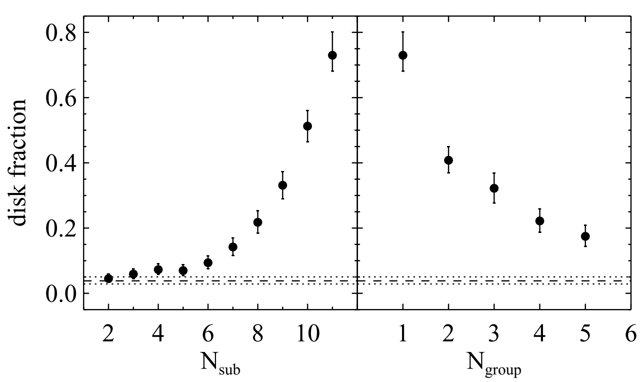

Figure 9. Left-hand panel: fraction of disc-like structures obtained in 10^5 realizations consisting $N_{\rm sub}$ subhaloes extracted from one group and $11 - N_{\rm sub}$ from the 'field'. Right-hand panel: fraction obtained when 11 subhaloes are extracted from $N_{\rm group}$ different groups. The fraction increases as more subhaloes from one group are selected, and as the number of groups contributing decreases. The likelihood of obtained a highly flattened distribution is always higher than when 11 subhaloes are randomly selected (dashed lines).

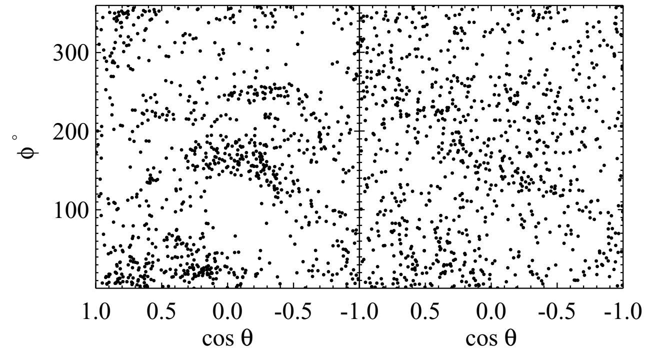

Figure 10. Present-time angular momentum orientation of subhaloes located within 300 kpc from the MW-like host. The left-hand panel shows the subhaloes from 'groups' while the right-hand panel corresponds to (a randomly selected subset from) the 'field'.

A second possibility is to consider only 'grouped' subhaloes, that is, we select randomly 11 subhaloes from $N_{\rm group}$ different groups where $N_{\rm group} = 1, \ldots, 5$. The panel on the right-hand side of Fig. 9 shows the fraction of disc-like configurations obtained in this way as a function of the number of groups considered. This fraction can be as high as $\sim$40 per cent when the subhaloes come from only two groups and, of course, reaches 73 per cent when they come from just one group. Note that the fraction when selecting from five different groups is still much higher than if one selects 11 subhaloes randomly.

The reason for the larger number of disc-like configurations when selecting subhaloes from several groups as in the right-hand panel of Fig. 9, rather than from just one group and the field, may be understood by examining Fig. 10. This shows the present-day angular momentum orientations for 'grouped' (left-hand panel) and 'field' (right-hand panel) subhaloes. The two distributions differ clearly in the sense that the 'grouped' subhaloes are generally more clustered (see also Section 2.2), also on larger scales. On the contrary, 'field' subhaloes tend to have their angular momenta more isotropically distributed. Therefore, when selecting 11 subhaloes purely from groups, the chance of picking up subhaloes with similar angular momentum orientations is higher than when selecting also from the 'field'. The more isotropically distributed orbits of 'field' subhaloes essentially add noise to the highly correlated orbits of subhaloes originating in just one group. Therefore, the disc signal gets smeared out quite significantly when more than half of the subhaloes are in the field in one realization, as shown on the left-hand panel of Fig. 9.

Given the large fraction of flattened configurations found in our simulations, we conclude that the spatial distribution of the 11 MW satellites can be reproduced within ΛCDM. The requirement is that these satellites fell on to the Galactic halo in groups.

3 DISCUSSION AND CONCLUSIONS

We have analysed a high-resolution cosmological simulation of the formation of a MW-like halo, focusing on the properties of the satellite population at the present day.

We have found that dark matter subhaloes are often accreted in groups in our simulations. Roughly one-third of the surviving subhaloes with mass $\geqslant 2.9 \times 10^6\,{\rm M}_\odot$ at the present epoch share this property. This is clearly a lower limit since we are not be able to

Downloaded from https://academic.oup.com/mnras/article-abstract/385/3/1365/1010777
by University of Groningen user
on 28 June 2018

identify accompanying haloes below our resolution limit (this is particularly severe at high redshift).

This group infall is apparent as an enhancement in the number of subhaloes whose angular momentum orientation is similar, particularly at the time of infall. This signal is measurable also from the present-day angular momentum of subhaloes, even for those accreted 8 Gyr ago. These groups of subhaloes share coherent orbits which can be traced back well before the accretion epoch. The differential group mass function follows a power-law distribution $\mathrm{d}N/\mathrm{d}\log M|_{\mathrm{group}} \propto M^n$ with $n \sim -0.5 \pm 0.2$. This is reminiscent of the differential mass function of subhaloes in both galaxy and cluster-size haloes, albeit with a shallower slope (compared to $n \sim -0.8$ as in e.g. De Lucia et al. 2004; Gao et al. 2004b).

We have also studied the degree of flattening of the spatial distribution of subhaloes in our simulation. The mean minor-to-major axis ratio c/a of the inertia tensor defined by the positions of 11-randomly selected subhaloes with 300 kpc is $c/a \sim 0.51 \pm 0.12$. In comparison, the c/a of the 11 'classical' MW satellites is 0.18 ± 0.01. Imposing the centrally concentrated MW satellite radial distribution leads to $c/a \sim 0.4 \pm 0.1$, and therefore somewhat alleviates the discrepancy with the observations (see also Kang et al. 2005).

We have explored also how this planar configuration may be obtained as a result of the infall of satellites in groups. The observed correlation in the angular momentum orientation of subhaloes naturally gives rise to disc-like configurations. For example, we find that if all subhaloes are accreted from just one group, it is almost impossible to avoid a disc-like distribution (∼80 per cent probability), while for accretion from just two groups, the likelihood of obtaining a distribution as planar as observed is 40 per cent.

These results may explain the origin of the ghostly streams proposed by Lynden-Bell & Lynden-Bell (1995). Out of the streams originally proposed, only two appear to have survived the rigour of time, after modern and accurate measurements of proper motions have become available. Palma et al. (2002) confirmed the LMC–SMC–UMi–Draco stream forms a kinematic group whose angular momentum separation is $<18\overset{\circ}{.}5$. More recently Piatek et al. (2005) ruled out with 95 per cent confident level UMi as a member using *HST* proper motions. The latest measurements of the Fornax proper motion by Piatek et al. (2007) have apparently confirmed the Sculptor–Sextans–Fornax stream (although previous measurements led to conflicting results, see Piatek et al. 2002; Dinescu et al. 2004). If some of the luminous satellites are embedded in dark (sub)haloes that fell in together, such coherent structures would be a naturally consequence of the hierarchical build up of galaxies.

In our simulations, such groups remain coherent in angular momentum (i.e. they share similar orbital planes giving rise to great circle streams) for approximately 8 Gyr. This implies that these groups (or satellites) should have been accreted by the MW at redshifts $z \sim 1$ or below.

One of the possible implications of the reality of the ghostly streams is that its member galaxies formed and evolved in a similar environment before falling into the MW potential. This would have implications on the (earliest) stellar populations of these objects, such as for example, sharing a common metallicity floor (Helmi et al. 2006). On the other hand, this implies that there should be groups that have not been able to host any luminous satellites. This would hint at a strong dependence on environment on the ability of a subhalo to retain gas (Scannapieco, Thacker & Davis 2001), or be shielded from reionization by nearby sources (Mashchenko, Carignan & Bouchard 2004; Weinmann et al. 2007).

Recent proper motion measurements of the Large and Small Magellanic Clouds (LMC and SMC) by Kallivayalil, van der Marel & Alcock (2006), as well as the simulations by Bekki & Chiba (2005) suggest that these systems may have become bound to each other only recently. This would be fairly plausible in the context of our results. The clouds may well have been part of a recently accreted group (see also Sales et al. 2007, for the link to Leo I) and it may not even be necessary for them to ever have been a binary system. This may also have implications on the computations of the past trajectories of these systems, particularly if both are embedded in a larger common dark matter envelope (Besla et al. 2007).

Our analysis shows that the dynamical peculiarities of the MW satellites can be understood in the context of the concordance cosmological model. Their properties must be a consequence of both the environment as well as of the hierarchical nature of the build up of galactic haloes.

ACKNOWLEDGMENTS

We thank Felix Stoehr for providing us with the GAnew simulations and for the great support in dealing with their analysis; Martin Smith and Simon White for stimulating discussions and suggestions. We are grateful to Laura Sales for a careful reading of the manuscript and for many useful discussions. We acknowledge financial support from the Netherlands Organization for Scientific Research (NWO).

REFERENCES

Bailin J., Steinmetz M., 2005, ApJ, 627, 647
Battaglia G. et al., 2005, MNRAS, 364, 433
Bekki K., Chiba M., 2005, MNRAS, 356, 680
Belokurov V. et al., 2006, ApJ, 647, L111
Belokurov V. et al., 2007, ApJ, 654, 897
Benson A. J., Frenk C. S., Lacey C. G., Baugh C. M., Cole S., 2002, MNRAS, 333, 177
Besla G., Kallivayalil N., Hernquist L., Robertson B., Cox T. J., van der Marel R. P., Alcock C., 2007, ApJ, 668, 949
Ciardi B., Stoehr F., White S. D. M., 2003, MNRAS, 343, 1101
De Lucia G., Kauffmann G., Springel V., White S. D. M., Lanzoni B., Stoehr F., Tormen G., Yoshida N., 2004, MNRAS, 348, 333
Dinescu D. I., Keeney B. A., Majewski S. R., Girard T. M., 2004, AJ, 128, 687
Dubinski J., Carlberg R. G., 1991, ApJ, 378, 496
Gao L., De Lucia G., White S. D. M., Jenkins A., 2004a, MNRAS, 352, L1
Gao L.,White S. D. M., Jenkins A., Stoehr F., Springel V., 2004b, MNRAS, 355, 819
Gilmore G., Wyse R. F. G., Norris J. E., 2002, ApJ, 574, L39
Helmi A. et al., 2006, ApJ, 651, L121
Irwin M. J. et al., 2007, ApJ, 656, L13
Kallivayalil N., van der Marel R. P., Alcock C., 2006, ApJ, 652, 1213
Kang X., Mao S., Gao L., Jing Y. P., 2005, A&A, 437, 383
Kauffmann G., White S. D. M., Guiderdoni B., 1993, MNRAS, 264, 201
Klypin A., Kravtsov A. V., Valenzuela O., Prada F., 1999, ApJ, 522, 82
Knebe A., Gill S. P. D., Gibson B. K., Lewis G. F., Ibata R. A., Dopita M. A., 2004, ApJ, 603, 7
Koch A., Grebel E. K., 2006, AJ, 131, 1405
Kravtsov A. V., Gnedin O. Y., Klypin A. A., 2004, ApJ, 609, 482
Kroupa P., 1997, New Astron., 2, 139
Kroupa P., Theis C., Boily M., 2005, A&A, 431, 517
Libeskind N. I., Frenk C. S., Cole S., Helly J. C., Jenkins A., Navarro J. F., Power C., 2005, MNRAS, 363, 146
Libeskind N. I., Cole S., Frenk C. S., Okamoto T., Jenkins A., 2007, MNRAS, 374, 16
Lynden-Bell D., Lynden-Bell R. M., 1995, MNRAS, 275, 429
Macció A. V., Moore B., Stadel J., Potter D., 2006, preprint (astro-ph/0609146)
McConnachie A. W., Irwin M. J., 2006, MNRAS, 365, 902

Downloaded from https://academic.oup.com/mnras/article-abstract/385/3/1365/1010777
by University of Groningen user
on 28 June 2018

Mashchenko S., Carignan C., Bouchard A., 2004, MNRAS, 352, 168
Mateo M., 1998, ARA&A, 36, 435
Metz M., Kroupa P., Jerjen H., 2007, MNRAS, 374, 1125
Moore B., Ghigna S., Governato F., Lake G., Quinn T., Stadel J., Tozzi P., 1999, ApJ, 524, L19
Palma C., Majewski S. R., Johnston K. V., 2002, ApJ, 564, 736
Piatek S. et al., 2002, AJ, 124, 3198
Piatek S., Pryor C., Bristow P., Olszewski E. W., Harris H. C., Mateo M., Minniti D., Tinney C. G., 2005, AJ, 130, 95
Piatek S., Pryor C., Bristow P., Olszewski E. W., Harris H. C., Mateo M., Minniti D., Tinney C. G., 2007, AJ, 133, 818
Sales L. V., Navarro J. F., Abadi M. G., Steinmetz M., 2007, MNRAS, 379, 1475
Scannapieco E., Thacker R. J., Davis M., 2001, ApJ, 557, 605
Simon J., Geha M., 2007, ApJ, 670, 313
Springel V., White S. D. M., Tormen G., Kauffmann G., 2001, MNRAS, 328, 726
Stoehr F., 2006, MNRAS, 365, 147
Stoehr F., White S. D. M., Tormen G., Springel V., 2002, MNRAS, 335, L84
Stoehr F., White S. D. M., Springel V., Tormen G., Yoshida N., 2003, MNRAS, 345, 1313
Taylor J. E., Babul A., Silk J., 2004, in Prada F., Martinez-Delgado D., Mahoney T. J., eds, ASP Conf. Ser. Vol. 327, Satellites and Tidal Streams. Astron. Soc. Pac., San Francisco, p. 205
Tormen G., Bouchet F. R., White S. D. M., 1997, MNRAS, 286, 865
Weinmann S. M., Macció A. V., Iliev I. T., Mellema G., Moore B., 2007, MNRAS, 381, 367
Willman B. et al., 2005a, ApJ, 626, L85
Willman B. et al., 2005b, AJ, 129, 2692
Zentner A. R., Kravtsov A. V., Gnedin O. Y., Klypin A. A., 2005, ApJ, 629, 219
Zucker D. B. et al., 2006a, ApJ, 643, L103
Zucker D. B. et al., 2006b, ApJ, 650, L41

This paper has been typeset from a TEX/LATEX file prepared by the author.

Downloaded from https://academic.oup.com/mnras/article-abstract/385/3/1365/1010777
by University of Groningen user
on 28 June 2018